Nonlinear planar Nernst effect in magnetic topological insulator heterostructures

Xin-Mei Wei ⬤, Ying-Li Wu ⬤, Jia-Liang Wan ⬤, and Xiao-Qin Yu ⬤ ,*
School of Physics and Electronics, Hunan University, Changsha 410082, China

A new nonlinear magnetothermal effect, namely nonlinear planar Nernst effect (NPNE), has been recently predicted in nonmagnetic topological insulators and Weyl semimetals. Both of the asymmetric energy dispersion and the in-plane magnetic field play significant roles in the reported materials. Here, we prove that the NPNE can also be generated in magnetic/nomagnetic topological heterostructures in the presence of an in-plane magnetization and in the absence of asymmetric energy dispersion. It is found that the NPNE has a quantum origin from the asymmetric magnon scattering and exhibits a cosine dependence on the orientation of the magnetization with respect to the direction of the temperature gradient (x direction).

I. INTRODUCTION

The three-dimensional (3D) topological insulators (TIs) [1,2], a new class of 3D materials with insulating bulk and conducting surface states, have played a significant role in many fields of condensed matter physics, such as spintronics [3–6] and quantum computation [1]. The spin directions of the surface Dirac electrons are locked perpendicularly to their momenta, namely spin-momentum locking [7,8], making TIs ideal spintronics materials and leading to highly efficient spin-to-charge conversion and magnetic switching. In addition, magnetic TIs provide an ideal platform to the realization of a system in which spin-polarized electrons interact with magnetism [9–13]. This offers a promising approach to addressing a crucial issue in the contemporary spintronics and spin caloritronics research [14–18]: the interaction of angular momentum between conduction electrons and local magnetization.

Owing to the interplay of the spin-momentum-locked surface states and magnetism, a series of magnetotransport phenomena are identified in magnetic TI films or bilayer structures composed of a ferromagnetic layer and a nonmagnetic TI layer. The identified magnetotransport phenomena include quantum anomalous Hall effect (QAHE) [19,20], bilinear magnetoresistance [21–23], unidirectional magnetoresistance (UMR) [13,24–27], unidirectional Seebeck effect (USE) [28,29], and current-nonlinear Hall effect (CNHE) [30]. Unlike intrinsic nonlinear thermoelectric effects originating from the band geometry (Berry curvature and Berry curvature dipole etc.,), such as nonlinear Hall effect [31–34] and nonlinear Nernst effect [35–38], these nonlinear magnetotransports require a magnetization or magnetic field coplanar with the driving forces (electric field or temperature gradient) and strongly depend on the orientation of magnetic field (or magnetization) with respect to driving forces.

Recently, a new nonlinear magnetothermal effect, namely the nonlinear planar Nernst effect (NPNE) [39,40], referring to a generation of the nonlinear Nernst current as a second-order response to the temperature gradient when the applied temperature gradient and the in-plane magnetic field (or magnetization) are coplanar [Fig. 1(b)], was first predicted in nonmagnetic TI Bi_2Te_3 and identified to originate from the conversion of a nonlinear transverse spin current to a charge current due to a combined result of hexagonal warping effect, spin-momentum locking, and the time-reversal symmetry breaking [39]. Being different from the relaxation-time dependence of nonlinear Nernst effect from band geometric properties as a response to the second order in temperature gradient: linear dependence of nonlinear anomalous Nernst effect (ANE) from the Berry curvature near the Fermi surface [36,37] and the independence of nonlinear intrinsic ANE attributed to the orbital magnetic quadrupole moment density (related to Berry phase) on the relaxation time [35], the NPNE in nonmagnetic TI stemming from the hexagonal warping effect exhibits a quadratic dependence on the relaxation time τ. Subsequently, NPNE has also been found to stem from chiral anomaly in Wely semimetals [40] and shows linear dependence on relaxation time. In those studies, the asymmetric energy dispersion, which is caused by the joint effect of in-plane magnetic field with hexagonal warping effect or chiral anomaly, plays a significant role to generate the nonlinear Nernst current. In this paper, we will show that the NPNE could also appear in TI heterostructure composed of nonmagnetic TI $(Bi_{1-y}Sb_y)_2Te_3$(BST) [41,42] and magnetic TI $Cr_x(Bi_{1-y}Sb_y)_{2-x}Te_3$ (CBST) [43,44] without considering the asymmetric energy dispersion. The finite NPNE in the heterostructure of BST/CBST is ascribed to the asymmetric magnon scattering, namely the asymmetric scattering of a conduction electron by a magnon due to the conservation of angular momentum [13] [Fig. 1(a)]. We find that the nonlinear Nernst current stemming from asymmetric magnon scattering as a response up to second order in temperature gradient could be easily distinguished from other contributions through a scaling relation with
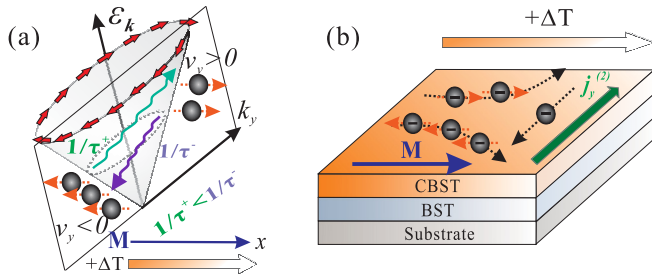

245422-1

FIG. 1. (a) The schematic illustration for the asymmetric magnon scattering of Dirac electron on the spin-momentum-locked Fermi surface. The black-dashed circle represents the Fermi surface. When the magnetization is in x direction, owing to spin-momentum locking effect and conservation of angular momentum during the magnon scattering process, the asymmetric relaxation time between the emission and absorption scattering processes will eventually lead to the imbalance of second-order electron distribution to temperature gradient between the electrons with the positive and negative group velocities in transverse direction (y direction) under temperature gradient, $\delta n_{2,v_y>0} \neq \delta n_{2,v_y<0}$. (b) Schematic diagram of the generation of nonlinear planar Nernst current $j_y^{(2)} \propto (\nabla_x T)^2$ driven by temperature gradient in presence of an in-plane magnetization **M** owing to asymmetric magnon scattering in (a). The direction of current is opposite to the electron moving direction.

the linear conductivity σ_{xx}: asymmetric magnon scattering (cubic to σ_{xx}), Berry curvature effect or chiral anomaly (linear to σ_{xx}), Berry phase effect (independent of σ_{xx}), and the warping effect or electron-hole asymmetry (quadratic to σ_{xx}). The general formula of nonlinear planar Nernst coefficient (NPNC) α_{nl}^P, quantizing the NPNE, is given in Sec. II. The Hamiltonian of heterostructure with coupling between surface Dirac electron and the magnetization is given in Sec. III. The expression of α_{nl}^P, stemming from the asymmetric magnon scattering, is deduced in Sec. IV. The behaviors and physics of NPNE for the heterostructure of BST/CBST are discussed in Sec. V. Finally, the conclusions are given in Sec. VI.

II. THE GENERAL FORMULA OF NONLINEAR PLANAR NERNST COEFFICIENT

The nonlinear planar Nernst effect can be characterized by the nonlinear planar Nernst coefficient (NPNC) α_{nl}^P (where the superscript "P" and subscript "nl" represent planar and nonlinear, respectively), which is defined as $j_y^{(2)} = \alpha_{nl}^P(\partial_x T)^2$ with $j_y^{(2)}$ indicating nonlinear transverse current density as a response to the second order in the longitudinal temperature gradient $\partial_x T$ in presence of an in-plane magnetic field or magnetization. The formulas of α_{nl}^P will be determined through the semiclassical Boltzmann equation within the relaxation time approximation as follows. The charge current density j_a in a direction is given by

$$j_a = -e \int [d\mathbf{k}] v_a f(\mathbf{r}, \mathbf{k}), \tag{1}$$

where $\int [d\mathbf{k}]$ is shorthand for $\int d\mathbf{k}/(2\pi)^2$, v_a represents the group velocity, and $f(\mathbf{r}, \mathbf{k})$ denotes the nonequilibrium distribution function. Within the relaxation time approximation, the Boltzmann equation for two-dimensional case in presence of

in-plane magnetic field and temperature gradient but without the external electric field is

$$-\frac{f - f_0}{\tau(\mathbf{k})} = \frac{\partial f}{\partial r_a} v_a, \tag{2}$$

where r_a indicates the a component of coordinate position of electron, $\tau(\mathbf{k})$ is the momentum-dependent relaxation time, and $f_0 = 1/[e^{(\epsilon_{\mathbf{k}}-E_f)/k_B T} + 1]$ represents the local equilibrium distribution function in which the energy correction (Zeeman term) induced by the in-plane magnetic field or magnetization has been considered in energy band $\epsilon_{\mathbf{k}}$. To determine the expression of current density j_a in Eq. (1) as a response up to the second order in temperature gradient, one would expand the nonequilibrium distribution function f as $f \approx f_0 + \delta f_1 + \delta f_2$ with the terms $\delta f_n \propto (\partial_a T)^n$ ($n > 2$) ignored due to small quantity $(\partial T/\partial r_a)^n$. After a tedious derivation in Appendix A, the formulas of the first-order (second-order) distribution function δf_1 (δf_2) to temperature gradient can be determined as follows:

$$\delta f_1 = \frac{\tau}{T\hbar}(\epsilon_{\mathbf{k}} - E_f)\frac{\partial f_0}{\partial k_a}\partial_a T,$$

$$\delta f_2 = \frac{\tau^2}{T\hbar}(\epsilon_{\mathbf{k}} - E_f)v_b\frac{\partial f_0}{\partial k_a}\left(\frac{2}{T}\partial_a T \partial_b T - \partial_{ab}T\right)$$

$$+ \frac{\tau^2}{\hbar^2 T^2}(\epsilon_{\mathbf{k}} - E_f)^2\frac{\partial^2 f_0}{\partial k_a \partial k_b}\partial_a T \partial_b T. \tag{3}$$

Therefore, when considering a uniform and single-directional temperature gradient applied along x direction, namely $\partial_{ab}T = 0$ and $a = b = x$ in Eq. (3), the thermally driven transverse charge current density $j_y^{(2)}$ [i.e., $a = y$ in Eq. (1)] as the second-order response to the temperature gradient $\partial_x T$ can be determined as $\alpha_{nl}^P(\partial_x T)^2$ with

$$\alpha_{nl}^P = -\frac{e}{\hbar^2 T^2}\int [d\mathbf{k}](\tau(\mathbf{k}))^2 v_y(\epsilon_{\mathbf{k}} - E_f)$$

$$\times \left[2v_x\hbar\frac{\partial f_0}{\partial k_x} + (\epsilon_{\mathbf{k}} - E_f)\frac{\partial^2 f_0}{\partial k_x^2}\right] \tag{4}$$

In previous studies, the relaxation time τ has been treated as a constant, and the nonvanishing nonlinear planar Nernst coefficient α_{nl}^P in presence of in-plane magnetic field strongly depends on the asymmetric energy dispersion ($\epsilon_{\mathbf{k}}$) stemming from the combined effect of in-plane magnetic field with hexagonal warping effect or chiral anomaly. In this paper, we find the nonvanishing α_{nl}^P in the TI heterostructure BST/CBST stems from the asymmetric magnon scattering [Fig. 1(b)]. For example, when the magnetization is along x direction, the localized spin of Cr is pointing in the $-x$ direction, meaning the angular momentum of magnon is $+1$. Therefore, owing to the angular momentum conservation, the electrons with spin parallel to magnetization (angular momentum $+1/2$) will be scattered to the states with spin antiparallel to magnetization ($-1/2$) by emitting a magnon. Meanwhile, because of the spin-momentum locking of TI, the electrons moving towards positive y axis ($v_y\hbar = \partial\epsilon_{\mathbf{k}}/\partial k_y > 0$) are scattered to states in which the electron flows towards negative y axis ($v_y < 0$) in the emission process. On the contrary, the electron scattered from negative group velocity and negative spin angular momentum ($v_y < 0$, $-1/2$) to positive velocity and spin ($v_y > 0$,

+1/2) must absorb a magnon owing to the conservation of angular momentum and the spin-momentum locking. The nonequivalence between the emission and absorption scattering processes leads to the asymmetry in relaxation time and eventually to the imbalance of electron distribution between the electrons with the positive and negative group velocities in transverse direction (y direction) under nonequilibrium conditions [Fig. 1(a)] owing to the spin-momentum locking effect of electron and the conservation of angular momentum during the magnon scattering process, giving rise to nonzero nonlinear planar Nernst coefficient $\alpha_{\mathrm{nl}}^{\mathrm{P}}$ (see details in Sec. IV) and nonlinear planar Nernst effect [Fig. 1(b)].

III. HAMILTONIAN FOR TI HETEROSTRUCTURE OF BST/CBST

In this paper, the NPNE will be investigated for the TI heterostructures BST/CBST, in which UMR has been observed experimentally [13] and USE was theoretically predicted [28]. Through tuning the composition y of element Sb, the Fermi energy E_f of the surface state can be modulated to locate inside the bulk band gap [13]. Hence, the carriers from the top and bottom surface states with a single Dirac cone will contribute to the conduction. Besides, in the presence of the heterostructure, only one surface involved in the MTI layer (i.e., CBST layer) will interact effectively with the magnetism. The effective Hamiltonian describing the surface Dirac electrons in the presence of in-plane magnetization $\mathbf{M}$ can be written as

$$H = H_0 + H', \tag{5}$$

where H_0 describes the Hamiltonian of the Dirac surface electrons when considering the coupling between the electron spin and the localized magnetic moment and has the following form [28]:

$$H_0 = (\mathbf{M} + v_F \hbar \mathbf{k} \times \hat{\mathbf{z}}) \cdot \boldsymbol{\sigma}$$
$$= (m \cos \phi + v_F \hbar k_y)\hat{\sigma}_x + (m \sin \phi - v_F \hbar k_x)\hat{\sigma}_y, \tag{6}$$

where v_F denotes the Fermi velocity, $\boldsymbol{\sigma} = (\hat{\sigma}_x, \hat{\sigma}_y, \hat{\sigma}_z)$ are Pauli matrices for the two basis functions of the energy band, $\hbar$ indicates the reduced Planck constant. In this paper, we consider the situation in which the magnetization orients in-plane, with $\mathbf{M} = (m_x, m_y) = m\mathbf{e}_m$ and $\mathbf{e}_m = (\cos \phi, \sin \phi)$, where the azimuth angle ϕ is measured from the direction of temperature gradient. It should be pointed out that, although the magnetization $\mathbf{M}$ of CBST initially points along the z direction, one would adjust the orientation of the magnetization $\mathbf{M}$ of CBST to the in-plane direction by applying an in-plane magnetic field $\mathbf{B}$ up to 0.7 T [13]. Yu *et al.* [39] showed that the contribution of electron-hole asymmetry to NPNE is insignificant and the hexagonal warping has a significant contribution to NPNE only when the Fermi energy is far away from the Dirac point. On the contrary, it is found that the asymmetric-magnon-scattering contribution to the nonlinear transports mainly appears around the Dirac point [13,28,30]. In addition, it is found that the contribution of asymmetric magnon scattering to the NPNE can be easily distinguished from the asymmetric energy dispersion through scaling relation (see details in Sec. IV). More importantly, a linear Dirac surface state, namely the absence of asymmetric energy

dispersion, would be achieved in the CBST when modulating the composition y of the element Sb and x of element Cr into appropriate value [10,43]. Therefore, for simplicity, the asymmetric energy dispersions, namely the electron-hole asymmetry (k^2 term) and hexagonal warping (k^3 term) in the surface state of BST/CBST, are reasonable to be neglected to disclose the behaviors of NPNE that stem from the asymmetric magnon scattering. The corresponding energy eigenvalues for H_0 are

$$\epsilon_\mathbf{k} = n\sqrt{(v_F \hbar k_x - m \sin \phi)^2 + (v_F \hbar k_y + m \cos \phi)^2}, \tag{7}$$

where $n(= \pm 1)$ is the band index. According to Eq. (7), one can easily notice that the shape of the linear Dirac cone remains unchanged, and only the Dirac point and the entire dispersion shift towards $\mathbf{e}_{k_m} = (\sin \phi, -\cos \phi)$ direction in momentum space when the magnetic field or magnetization is located in the $\mathbf{e}_m$ direction. In addition, based on Eq. (6), one would further confirm that the considered surface states hold two mirror lines (namely $k_x = m \sin \phi / v_F \hbar$, and $k_y = -m \cos \phi / v_F \hbar$) in the presence of magnetization, which guarantee there is no nonlinear Nernst current stemming from the band geometries generated. That is because the largest symmetry of a 2D system allows for the nonvanishing nonlinear ANE is a single mirror line [36] and the nonlinear intrinsic ANE disappears due to the existence of two mirror lines in the system [35]. The second term of the Hamiltonian, namely H', means the interaction between the surface conduction electrons and the localized spin composed of Cr d orbits (magnon) and can be determined through conservation of the angular momentum as [13]

$$H' \approx \sum_i j_{\mathrm{ex}}(c_{i,\uparrow}^\dagger c_{i,\downarrow} b_i + c_{i,\downarrow}^\dagger c_{i,\uparrow} b_i^\dagger)$$
$$= \frac{1}{\sqrt{N}} \sum_{\mathbf{k},\mathbf{q}} j_{\mathrm{ex}}(c_{\mathbf{k+q},\uparrow}^\dagger c_{\mathbf{k},\downarrow} b_\mathbf{q} + c_{\mathbf{k-q},\downarrow}^\dagger c_{\mathbf{k},\uparrow} b_\mathbf{q}^\dagger), \tag{8}$$

where N is the number of lattice unit cells [45,46], j_{ex} represents the exchange-coupling constant, and $b^\dagger(b)$ and $c^\dagger(c)$ indicate the creation (annihilation) operator of the magnon and surface Dirac electron, respectively. The first (second) term in the bracket of the second line in Eq. (8) describes the magnon absorption (emission) process. In the absorption process $(c_{\mathbf{k+q},\uparrow}^\dagger c_{\mathbf{k},\downarrow} b_\mathbf{q})$, when the system absorbs a magnon with momentum $\mathbf{q}$, the Dirac electron in surface state $|\mathbf{k}, \downarrow\rangle$ will be scattered to the state $|\mathbf{k} + \mathbf{q}, \uparrow\rangle$ with a momentum increase $\mathbf{q}$ due to the conservation of the momentum and a spin reversion from $\downarrow (s_\phi = -1/2)$ to $\uparrow (s_\phi = 1/2)$ resulting from the conservation of angular momentum and the spin-momentum locking of the surface Dirac state. In the emission process $(c_{\mathbf{k-q},\downarrow}^\dagger c_{\mathbf{k},\uparrow} b_\mathbf{q}^\dagger)$, on the contrary, the electron spin will be reversed from $\uparrow$ to $\downarrow$ and the momentum is reduced from $\mathbf{k}$ to $\mathbf{k} - \mathbf{q}$ by emitting a magnon with $\mathbf{q}$.

IV. THE ASYMMETRIC-MAGNON-SCATTERING-INDUCED NPNE

Taking into account the magnon scattering and assuming that the magnon scattering is independent of other types of scattering processes such as impurities, phonons, electron-

electron for simplicity [28], the relaxation time is

$$\frac{1}{\tau(\mathbf{k})} = \frac{1}{\tau^0} + \frac{1}{\tau_{\text{mag}}(\mathbf{k})}, \tag{9}$$

where τ^0 is nonmagnetic scattering relaxation time and τ_{mag} is the relaxation time scattered by magnons. When the impurity scattering is dominant, which means $\tau^0 \ll \tau_{\text{mag}}$, the relaxation time $\tau(\mathbf{k})$ can be approximated to the first order as $\tau(\mathbf{k}) \approx \tau^0 - (\tau^0)^2/\tau_{\text{mag}}(\mathbf{k})$. Therefore, the nonlinear Nernst coefficient α_{nl}^P in Eq. (4) can be further expressed as

$$\alpha_{\text{nl}}^P = -e(\tau^0)^2 \int [d\mathbf{k}] v_y \left\{ \left[2v_x \frac{\epsilon_{\mathbf{k}} - E_f}{\hbar T^2} \frac{\partial f_0}{\partial k_x} + \right. \right.$$
$$\left. + \left(\frac{\epsilon_{\mathbf{k}} - E_f}{\hbar T} \right)^2 \frac{\partial^2 f_0}{\partial k_x^2} \right] - \frac{2\tau^0}{\tau_{\text{mag}}(\mathbf{k})} \left[2v_x \frac{\epsilon_{\mathbf{k}} - E_f}{\hbar T^2} \frac{\partial f_0}{\partial k_x} \right.$$
$$\left. \left. + \left(\frac{\epsilon_{\mathbf{k}} - E_f}{\hbar T} \right)^2 \frac{\partial^2 f_0}{\partial k_x^2} \right] \right\}, \tag{10}$$

showing that there are two distinguishing mechanisms giving rise to nonlinear Nernst effect, namely the asymmetric energy dispersion (the first term) and the asymmetric magnon scattering (the second term). In this paper, we only consider the nonlinear Nernst effect induced by the asymmetric magnon scattering, namely

$$\alpha_{\text{nl,(mag)}}^P = 2e(\tau^0)^3 \int [d\mathbf{k}] \frac{1}{\tau_{\text{mag}}(\mathbf{k})} \left[2v_x v_y \frac{\epsilon_{\mathbf{k}} - E_f}{\hbar T^2} \frac{\partial f_0}{\partial k_x} \right.$$
$$\left. + v_y \left(\frac{\epsilon_{\mathbf{k}} - E_f}{\hbar T} \right)^2 \frac{\partial^2 f_0}{\partial k_x^2} \right]. \tag{11}$$

Actually, through exploiting the parities (see details in Appendix D), one can easily find that the term in the first bracket in Eq. (10) is zero for the system whose energy dispersion has the formula as Eq. (7). Based on the Fermi's golden rule and the interaction between the electrons and magnons [Eq. (8)], the magnon relaxation time $\tau_{\text{mag}}(\mathbf{k})$ in Eq. (11) can be determined as (details can be found in the literatures [13,28] and also in the Appendix C)

$$\frac{1}{\tau_{\text{mag}}(\alpha, \Delta k)} = \frac{1}{\tau_F^m} \int_0^{2\pi} d\theta \cos^2\left(\frac{\pi}{4} + \frac{\alpha - \phi}{2} \right) \sin^2\left(\frac{\pi}{4} + \frac{\theta - \phi}{2} \right) V_{\text{mag}}^+(\theta, \alpha, \Delta k) + \sin^2\left(\frac{\pi}{4} + \frac{\alpha - \phi}{2} \right)$$
$$\times \cos^2\left(\frac{\pi}{4} + \frac{\theta - \phi}{2} \right) V_{\text{mag}}^-(\theta, \alpha, \Delta k), \tag{12}$$

with $\frac{1}{\tau_F^m} = \frac{k_F j_{\text{ex}}^2 A_c}{2\pi v_F \hbar^2}$, where the $k_F = E_f/\hbar v_F$ is the Fermi momentum and in-plane unit-cell area $A_c = 3\sqrt{3}a^2/2$ is determined by the hexagonal lattice constant a, and

$$V_{\text{mag}}^+ = \frac{1}{e^{\hbar\omega\beta} - 1} \left(1 - \frac{1}{e^{\beta(\hbar\omega + \hbar v_F \Delta k)} + 1} \right), \tag{13}$$

$$V_{\text{mag}}^- = \frac{e^{\hbar\omega\beta}}{e^{\hbar\omega\beta} - 1} \left(1 - \frac{1}{e^{\beta(\hbar v_F \Delta k - \hbar\omega)} + 1} \right), \tag{14}$$

where Δk is the radius measured from k_F [Eq. (C8)], α (θ) are the polar angles of the initial (final) electrons, and $\hbar\omega$ corresponds to the magnon energy with $2k_F \sin\left(\frac{\theta - \alpha}{2}\right)$ wave number. V_{mag}^+ (V_{mag}^-) is relevant to the magnon absorption (emission) process. The first factors of Eqs. (13) and (14) represent the probability of magnon absorption and emission, respectively, and the second ones show the probability that the final state of the electrons is unoccupied. The magnon band dispersion in the long-wave-number situation is given by [47]

$$\hbar\omega = 4D_s k_F^2 \sin^2\left(\frac{\theta - \alpha}{2} \right) + g\mu_B B, \tag{15}$$

where D_s denotes the spin stiffness constant and the Landé factor g is approximately equal to 2 in CBST. Combining the band energy $\epsilon_{\mathbf{k}}$ [Eq. (7)] with magnon relaxation time $\tau_{\text{mag}}(\mathbf{k})$ in Eq. (12), the formula of the nonlinear Nernst coefficient α_{nl}^P

is found to be

$$\alpha_{\text{nl}}^P = \frac{\gamma E_f^2}{T} \int\int\int dx d\alpha d\theta V_{\text{mag}}\left(\theta, \alpha, \phi, \frac{k_B T x}{\hbar v_F} \right)$$
$$\times \frac{x e^x \cos^2\alpha \sin\alpha}{(e^x + 1)^2} \left(\frac{x e^x - x}{e^x + 1} - 2 \right), \tag{16}$$

where V_{mag} is given in Eq. (C13), $x = \hbar v_F \Delta k / k_B T$ is a dimensionless integral variable, and $\gamma = e j_{\text{ex}}^2 k_B (\tau^0)^3 A_c / (4\pi^3 \hbar^5 v_F)$ is a typical scale for heterostructures BST/CBST. Obviously, this α_{nl}^P stemming from asymmetric magnon scattering shows cubic dependence on the relaxation time τ^0, hinting $\alpha_{\text{nl}}^P \propto \sigma_{xx}^3$, where $\sigma_{xx}(\propto \tau^0)$ denotes the longitudinal conductivity. Therefore, one would easily distinguish the asymmetric-magnon-scattering contribution to nonlinear Nernst current from other mechanisms through a scaling relation: asymmetric magnon scattering (cubic to σ_{xx}), Berry curvature effect or chiral anomaly (linear to σ_{xx}), Berry phase effect (independent

of σ_{xx}), and the warping effect or electron-hole asymmetry (quadratic to σ_{xx}).

The microscopic mechanism of the asymmetric-magnon-scattering-induced NPNE can, actually, be disclosed intuitively through neglecting the magnon dispersion, which means $\hbar\omega \approx g\mu_B B$. When neglecting the magnon dispersion and using $g\mu_B B$ as the magnon energy, the integral involving the angular variables in Eq. (16), then, can be integrated out, leading to

$$\alpha_{nl}^P = -\frac{\gamma\pi^2 E_f^2 \tau_F^m}{8T}\cos\phi \int dx \left(\frac{1}{\tau^+} - \frac{1}{\tau^-}\right)$$
$$\times \frac{xe^x}{(e^x+1)^2}\left(\frac{xe^x - x}{e^x + 1} - 2\right), \tag{17}$$

with the definitions of τ^+ and τ^- given as [13,28]

$$\frac{1}{\tau^+} = \frac{1}{e^{\beta\hbar\omega}-1}\left(1 - \frac{1}{e^{(x+\beta\hbar\omega)}+1}\right)\frac{1}{\tau_F^m},$$
$$\frac{1}{\tau^-} = \left(\frac{1}{e^{\beta\hbar\omega}-1}+1\right)\left(1 - \frac{1}{e^{(x-\beta\hbar\omega)}+1}\right)\frac{1}{\tau_F^m}, \tag{18}$$

where $1/\tau_F^m = k_F j_{ex}^2 A_c/(2\pi v_F \hbar^2)$, which ensures τ^+ and τ^- having the dimensions of the relaxation time. Obviously, the scattering rate $1/\tau^+$ for absorbing a magnon with energy $\hbar\omega$ is not equal to the scattering rate $1/\tau^-$, which corresponds to emitting a magnon with same energy. Therefore, Eq. (17) hints nonzero NPNE, which originates from the asymmetric magnon scattering of electron in the TI, namely, the scattering rates are different in magnon absorption and emission processes. Besides, Eq. (17) also exhibits $\cos\phi$ dependence on the magnetization orientation. It should be pointed out that the $\cos\phi$ dependence still holds even when considering magnon dispersion as shown in Fig. 2(a) from numerical calculations. Therefore, $|\alpha_{nl}^P|$ reaches its maximum value when **M** is parallel or antiparallel to the applied temperature gradient (x axis) and vanishes when **M** is vertical to the temperature gradient. This $\cos\phi$ dependence might be attributed to the fact that only $m_x(\propto \cos\phi)$ component of **M** can lead to an antisymmetric magnon scattering while the m_y component induces symmetric magnon scattering in the transverse transport process, namely, the carriers flowing perpendicularly to the driving force (see details in Appendix E). Actually, the magnetization component contributing to symmetric or antisymmetric magnon scattering in transverse transport process are opposite to the longitudinal process in which the m_x (m_y) component of magnetization contributes to symmetric (antisymmetric) scattering, leading to a $\sin\phi$ dependence (measured from x direction) of the USE on the orientation of magnetization [28].

V. RESULTS AND DISCUSSION

To numerically analyze the behaviors of the NPNE, which stems from asymmetric magnon scattering in TI heterostructures BST/CBST without neglecting the magnon dispersion, we use the following typical values: the lattice constant $a = 4.383\,\text{Å}$ [48,49], the Fermi velocity $v_F \approx 1 \times 10^5\,\text{m/s}$ [50], spin stiffness constant $D_s \approx 2.1 \times 10^{-22}\,\text{eV m}^2$ [47], and the nonmagnetic scattering relaxation time $\tau^0 \approx 5 \times 10^{-13}\,\text{s}$ estimated by $\tau^0 = \mu m/e$. The mobility μ of $(Bi_{1-y}Sb_y)_2Te_3$ with Cr doping on the surface can range

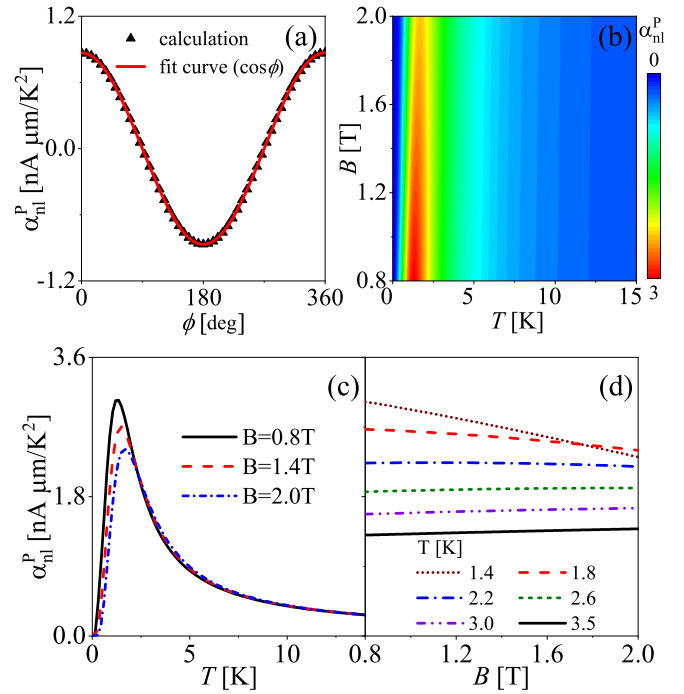FIG. 2. (a) The dependence of α_{nl}^P on in-plane magnetization orientation (i.e., ϕ). (b) α_{nl}^P as a function of temperature T and magnetic field B. (c) α_{nl}^P vs T for different B. (d) α_{nl}^P vs B for different T. The angle $\phi = 0$ (namely, the direction of magnetization is aligned to the temperature gradient) and $E_f = 50\,\text{meV}$ are fixed in (b)–(d).

from 200 to $2250\,\text{cm}^2\,\text{V}^{-1}\,\text{s}^{-1}$ [51], $\mu = 1500\,\text{cm}^2\,\text{V}^{-1}\,\text{s}^{-1}$ is taken for an estimation here. Since the exchange coupling constant j_{ex} is not well known for BST/CBST heterostructure, here we adopt a typical value ($j_{ex} \approx 0.1\,\text{eV}$) [52] for the exchange coupling constant of surface states of Sb_2Te_3 and impurities. Hence, the typical scale γ is found to be $5.64 \times 10^{-12}\,\text{Am/[K (eV)}^2]$. The maxima of α_{nl}^P are expected in the relatively lower temperature and weaker magnetic field [Fig. 2(b)].

Figure 2(c) displays the temperature dependence of α_{nl}^P for different magnetic fields. The appearance of a peak [Fig. 2(c)] can be understood as follows: When the temperature T tends to be zero or say in the extremely low temperature regime $k_B T \ll \hbar\omega_{min}$ ($\hbar\omega_{min} = g\mu_B B$), namely, $T = 1.34\,K$ for $B = 1\,T$, α_{nl}^P will tend to be zero owing to the frozen magnons. On the other hand, at relatively high temperature $k_B T \gg \hbar\omega_{max}$ (the maximum energy of magnon $\hbar\omega_{max}$ is $4D_s k_F^2 + g\mu_B B$), the nonlinear Nernst coefficient α_{nl}^P exhibits an inverse-linear dependence on temperature ($\alpha_{nl}^P \propto 1/T$). As a result, a peak will emerge at an intermediate temperature. It's also found that the amplitude of the peak becomes smaller and the position shifts to higher temperature when the magnetic field increases. Furthermore, the value of α_{nl}^P is insensitive to the magnetic field in the high-temperature regime.

Actually, the temperature-dependent behaviors of the NPNE in both extremely low- and high-temperature regime could be understood qualitatively when ignoring the magnon dispersion for a more transparent picture. At the extremely low temperature ($k_B T \ll \hbar\omega_{min}$), we have $1/\tau^+ \approx e^{-\beta\hbar\omega}/\tau_F^m$ and $1/\tau^- \approx 0$. Consequently, the temperature dependence
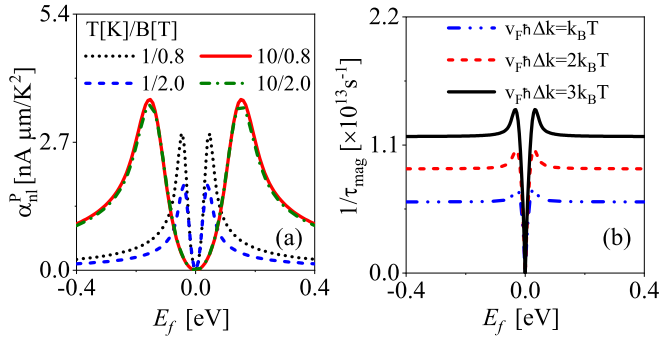
FIG. 3. (a) The Fermi energy dependence of α_{nl}^P for different T and B. (b) The magnon scattering rate $1/\tau_{mag}$ as a function of Fermi energy for different Δk. The magnetic field and temperature in (b) are fixed at 0.8 T and 1.0 K, respectively. Both orientations of magnetization are along the direction of temperature gradient (namely, $\phi = 0$) in (a) and (b).

of α_{nl}^P behaves as $\alpha_{nl}^P \propto e^{-\beta\hbar\omega}/T$. Since $e^{\beta\hbar\omega}$ diverges much faster than $1/T$, α_{nl}^P will tend to be zero. In the considered high-temperature regime, hinting $\beta\hbar\omega \to 0$, the inverse of the number of the magnon shows an inverse-linear dependence on T ($1/n_B \approx \hbar\omega/k_BT$) and the difference $\Delta f_{2\hbar\omega}$ between $1/[\exp(x + \beta\hbar\omega) + 1]$ and $1/[\exp(x - \beta\hbar\omega) + 1]$ manifests itself as inversely dependent on T [$\Delta f_{2\hbar\omega} = -2\hbar\omega e^x(1 + e^x)^{-2}/k_BT$]. Hence, the difference of $1/\tau^+ - 1/\tau^-$ ($= -\Delta f_{2\hbar\omega} \cdot n_B \cdot \frac{1}{\tau_F^m}$) in Eq. (17) is independent of T, leading to the nonlinear Nernst coefficient inverse-linear dependence on temperature, namely, $\alpha_{nl}^P \propto 1/T$.

Figure 2(d) shows the dependence of α_{nl}^P on magnetic field B for different temperature. It should be pointed out that since we only consider the small magnetic field [$B \leqslant 2\,\text{T}$] in this paper, the Landau level would be ignored. At low temperature, for example $T = 1.4\,\text{K}$ [Fig. 2(d)], it is easy to observe that α_{nl}^P linearly decreases as the magnetic field increases. This reducing behavior of α_{nl}^P versus B at low temperature might be explained as follows. With the magnetic field B increasing, the energy of magnon [Eq. (15)] enhances. As a result, the population of magnon decreases at the fixed temperature in the low-temperature regime, leading to the decrease of α_{nl}^P. However, as the temperature continues to increase, the impact of varying the magnetic field becomes insignificant on α_{nl}^P [Figs. 2(c) and 2(d)], which might be due to the fact that the enhanced thermal motion with temperature increase would be large enough to make almost all the magnons to be excited.

Figure 3(a) illustrates the dependence of α_{nl}^P on the Fermi energy at different temperature and magnetic field values and shows the particle-hole symmetry, which is evident since α_{nl}^P is an even function of E_f. Obviously, the values of the asymmetric-magnon-scattering-induced α_{nl}^P mainly appear at low Fermi energy close to Dirac cone. Therefore, in addition to the scaling relation, the Fermi energy dependence of NPNE can also be used to distinguish the asymmetric magnon scattering from the warping-effect contribution since the warping-effect contribution becomes significant only when the Fermi energy is far away from Dirac point [39]. The peak feature [Fig. 3(a)] can be interpreted as the combined effect of the magnon population and the density of states of the charge carriers [28]. When increasing the absolute value of

Fermi energy E_f, the density of states of carriers increases and the related magnon population, conversely, decreases owing to the increase of energy of magnon contributing to the scattering process. As a result, the magnon scattering rate $1/\tau_{mag}$ [Fig. 3(b)] increases rapidly first due to the enhancement of density of states and then decreases since the magnon population decreases, leading to the peak feature (α_{nl}^P vs E_f). It is also observed that the curves with different B almost overlap at low Fermi level $|E_f|$ with a fixed temperature, meaning an insignificant impact of the magnetic field on α_{nl}^P. However, when E_f continues to increase and is away from the Dirac cone, α_{nl}^P will decrease with an increasing B.

To numerically estimate the nonlinear NPNE of the BST/CBST heterostructures, we take $\alpha_{nl}^P \approx 3.6\,\text{nA}\,\mu\text{m}\,\text{K}^{-2}$ [Fig. 3(a)] for $T = 10\,\text{K}$, $B = 0.8\,\text{T}$, and $E_f = 0.15\,\text{eV}$. The temperature gradient $\partial_x T$ can already reach $1\,\text{K}\,\mu\text{m}^{-1}$ in experiment [53]. Hence, the nonlinear charge current $j_y^{(2)}l = \alpha_{nl}^P l(\partial_x T)^2$ can reach $0.18\,\mu\text{A}$ with the length of sample $l = 50\,\mu\text{m}$, which is in the same order of magnitude that stemmed from the asymmetric energy dispersion in nonmagnetic TI Bi$_2$Te$_3$ [39] and measurable [54]. Essentially, the proposed asymmetric-magnon-scattering NPNE here could be expected to appear in systems, which follow two requisites: (1) the spin-momentum locking of surface states; (2) magnetic elements with the local spin in plane, hinting in-plane magnetization. Therefore, one would also expect to observe the asymmetric-magnon-scattering NPNE in VBST/BST heterostructures by replacing Cr doping with V doping.

VI. CONCLUSIONS

In summary, we have proposed that a nonlinear planar Nernst effect (NPNE) can also emerge in the heterostructures of TI/MTI without considering the asymmetric energy dispersion. This NPNE can be ascribed to the asymmetric magnon scattering, namely the differing scattering rate for absorption process and emission process. The magnitude of nonlinear planar Nernst current in BST/CBST heterostructure is comparable to that predicted in nonmagnetic TI Bi$_2$Te$_3$, which is attributed to the asymmetric energy dispersion. The nonlinear planar Nernst coefficient α_{nl}^P, quantizing NPNE, has been determined through the semiclassical Boltzmann equation within the relaxation time approximation and shows a $\cos\phi$ dependence on the orientation of the magnetization with respect to the direction of temperature gradient. It is also found that a stronger NPNE occurs at relatively lower temperature ($k_BT \ll g\mu_B B$) and weaker magnetic field. At relatively high temperature ($k_BT \gg 4D_s k_F^2 + g\mu_B B$), α_{nl}^P shows an inverse-linear dependence on temperature and is independent of the magnetic field. Besides, α_{nl}^P displays the particle-hole symmetry, namely the sign and magnitude keep unchanging when transferring the system from p doping to n doping.

ACKNOWLEDGMENTS

APPENDIX A: THE NONEQUILIBRIUM DISTRIBUTION FUNCTION

Within the relaxation time approximation, the Boltzmann equation for two-dimensional case in presence of in-plane magnetic field and temperature gradient but without the external electric field is

$$f - f_0 = -\tau \frac{\partial f}{\partial r_a} v_a. \tag{A1}$$

We treat the temperature gradient ∇T as a small quantity and expand the local nonequilibrium distribution function $f(\mathbf{r}, \mathbf{k})$ in terms of ∇T up to the second order as

$$f(\mathbf{r}, \mathbf{k}) \approx f_0(\mathbf{r}, \mathbf{k}) + \delta f_1(\partial_a T) + \delta f_2(\partial_a T \partial_b T), \tag{A2}$$

where f_0 is the local equilibrium distribution function depending on $\mathbf{r}$ and $\mathbf{k}$ via indirect variables T and $\epsilon_\mathbf{k}$ as $f_0(\mathbf{r}, \mathbf{k}) = f_0(\epsilon(\mathbf{k}), T(\mathbf{r}))$, where the energy dispersion $\epsilon_\mathbf{k}$ includes the energy-correction (Zeeman term) stemmed from the in-plane magnetic field or magnetization, leading to the following partial derivative relations:

$$\frac{\partial f_0}{\partial r_a} = \frac{\partial f_0}{\partial T} \frac{\partial T}{\partial r_a}, \quad \frac{\partial f_0}{\partial k_a} = \frac{\partial f_0}{\partial \epsilon_\mathbf{k}} \frac{\partial \epsilon_\mathbf{k}}{\partial k_a}. \tag{A3}$$

By directly differentiating f_0 with respect to $\epsilon_\mathbf{k}$ and T, one can find

$$\frac{\partial f_0}{\partial T} = -\frac{\epsilon_\mathbf{k} - E_f}{T} \frac{\partial f_0}{\partial \epsilon_\mathbf{k}}. \tag{A4}$$

Combining Eqs. (A3) and (A4) with the definition of electron velocity $\nabla_\mathbf{k} \epsilon_\mathbf{k} = \hbar \mathbf{v}$, we have

$$\frac{\partial f_0}{\partial k_a} = -\frac{\partial f_0}{\partial T} \frac{\hbar T v_a}{\epsilon_\mathbf{k} - E_f}. \tag{A5}$$

Taking the expansion of f in Eq. (A2) into Eq. (A1) and comparing the order of temperature gradient for both sides of the equation, we can obtain

$$\delta f_1 = -\tau \frac{\partial f_0}{\partial T} v_a \partial_a T,$$
$$\delta f_2 = \tau^2 \left(\frac{\partial^2 f_0}{\partial T^2} \partial_a T \partial_b T + \frac{\partial f_0}{\partial T} \partial_{ab} T \right) v_b v_a. \tag{A6}$$

To obtain Eq. (A6), we have used the first relation in Eq. (A3) and also introduce the shorthand notations, $\partial_a = \partial/\partial r_a$, $\partial_{ab} = \partial^2/\partial r_a \partial r_b$. Based on Eqs. (A5) and (A6), we find

$$\delta f_1 = \frac{\tau}{T\hbar}(\epsilon_\mathbf{k} - E_f) \frac{\partial f_0}{\partial k_a} \partial_a T,$$

$$\delta f_2 = -\frac{\tau^2}{T\hbar}(\epsilon_\mathbf{k} - E_f) v_b \frac{\partial f_0}{\partial k_a} \left(\partial_{ab} T - \frac{2}{T} \partial_a T \partial_b T \right)$$

$$+ \frac{\tau^2}{\hbar^2 T^2}(\epsilon_\mathbf{k} - E_f)^2 \frac{\partial^2 f_0}{\partial k_a \partial k_b} \partial_a T \partial_b T. \tag{A7}$$

It should be pointed out that one has $\partial_{ab} T = 0$ in a uniform temperature gradient. In addition, owing to the presence of in-plane magnetic field or magnetization, when calculating the energy dispersion $\epsilon_\mathbf{k}$, one needs to take into account the energy correction (Zeeman term) caused by the in-plane magnetic field or magnetization.

APPENDIX B: THE THERMALLY DRIVEN NONLINEAR CHARGE CURRENT

Based on Eq. (A7), the a component of thermally driven charge current density $j_a = -e \int [d\mathbf{k}] v_a f(\mathbf{r}, \mathbf{k})$ as response up to second order in temperature gradient is found to be

$$j_a = -\frac{e}{\hbar T} \partial_b T \int [d\mathbf{k}] \tau v_a (\epsilon_\mathbf{k} - E_f) \frac{\partial f_0}{\partial k_b}$$

$$- e \partial_b T \partial_c T \int [d\mathbf{k}] \tau^2 \left[2v_a v_c \frac{\epsilon_\mathbf{k} - E_f}{\hbar T^2} \frac{\partial f_0}{\partial k_b} \right.$$

$$\left. + v_a \left(\frac{\epsilon_\mathbf{k} - E_f}{\hbar T} \right)^2 \frac{\partial^2 f_0}{\partial k_b \partial k_c} \right]$$

$$+ \frac{e}{\hbar T} \partial_{bc} T \int [d\mathbf{k}] \tau^2 v_a v_b (\epsilon_\mathbf{k} - E_f) \frac{\partial f_0}{\partial k_c}. \tag{B1}$$

When applying the temperature gradient along x direction (i.e., $b = c = x$), the current density j_y in y direction (i.e., $a = y$) is found to be

$$j_y = -\frac{e}{\hbar T} \partial_x T \int [d\mathbf{k}] \tau v_y (\epsilon_\mathbf{k} - E_f) \frac{\partial f_0}{\partial k_x}$$

$$+ \frac{e}{\hbar T} \partial_x^2 T \int [d\mathbf{k}] \tau^2 v_y v_x (\epsilon_\mathbf{k} - E_f) \frac{\partial f_0}{\partial k_x}$$

$$- e(\partial_x T)^2 \int [d\mathbf{k}] \tau^2 \left[2v_y v_x \frac{\epsilon_\mathbf{k} - E_f}{\hbar T^2} \frac{\partial f_0}{\partial k_x} \right.$$

$$\left. + v_y \left(\frac{\epsilon_\mathbf{k} - E_f}{\hbar T} \right)^2 \frac{\partial^2 f_0}{\partial k_x^2} \right]. \tag{B2}$$

Combining with the definition of coefficient $[\alpha_{nl}^P = j_y^{(2)}/(\partial_x T)^2]$, the formula of the nonlinear Nernst coefficient α_{nl}^P can be easily determined and given in Eq. (4).

APPENDIX C: MAGNON RELAXATION TIME τ_{mag} AND NONLINEAR PLANAR NERNST COEFFICIENT α_{nl}^P OF BST/CBST

In this Appendix, the magnon relaxation time τ_{mag} [13,28] will be determined based on the Fermi's golden rule,

$$\frac{1}{\tau_{mag}(\mathbf{k})} \approx \sum_{\mathbf{k}'} W_{mag}(\mathbf{k}'|\mathbf{k})(1 - f(\mathbf{k}')), \tag{C1}$$

with

$$W_{mag}(\mathbf{k}'|\mathbf{k}) = W_{abs}(\mathbf{k}', \sigma'; n_{\mathbf{k}'-\mathbf{k}} - 1 | \mathbf{k}, \sigma; n_{\mathbf{k}'-\mathbf{k}})$$
$$+ W_{emit}(\mathbf{k}', \sigma'; n_{\mathbf{k}-\mathbf{k}'} + 1 | \mathbf{k}, \sigma; n_{\mathbf{k}-\mathbf{k}'}), \tag{C2}$$

where $1 - f(\mathbf{k}')$ is the probability that the final state of electron is unoccupied. The scattering probabilities W_{abs} (W_{emit}) of magnon absorption (emission) process are expressed as

$$W_{abs} = \frac{2\pi}{\hbar} |\langle \mathbf{k}', \sigma'; n_{\mathbf{k}'-\mathbf{k}} - 1 | H' | \mathbf{k}, \sigma; n_{\mathbf{k}'-\mathbf{k}} \rangle|^2$$
$$\times \delta(\epsilon_{\mathbf{k}'} - \epsilon_\mathbf{k} - \hbar\omega_{\mathbf{k}'-\mathbf{k}}),$$

$$W_{emit} = \frac{2\pi}{\hbar} |\langle \mathbf{k}', \sigma'; n_{\mathbf{k}-\mathbf{k}'} + 1 | H' | \mathbf{k}, \sigma; n_{\mathbf{k}-\mathbf{k}'} \rangle|^2$$
$$\times \delta(\epsilon_{\mathbf{k}'} - \epsilon_\mathbf{k} + \hbar\omega_{\mathbf{k}-\mathbf{k}'}), \tag{C3}$$

where $\mathbf{k}, \sigma$ and $\mathbf{k}', \sigma'$ represent the wave vectors and spins of initial and final state of electron, respectively, $n_{\mathbf{k}} = 1/e^{\beta\hbar\omega_{\mathbf{k}}} - 1$ denotes the number of magnons with wave vector $\mathbf{k}$, and $\hbar\omega$ corresponds to the magnon energy. Taking the interaction Hamiltonian H' given in Eq. (8) into Eq. (C3), yields

$$W_{abs} = \frac{2\pi}{\hbar} \frac{j_{ex}^2}{N} n_{\mathbf{k}'-\mathbf{k}} \mid \langle \sigma' \mid c_{\uparrow}^{\dagger} c_{\downarrow} \mid \sigma \rangle \mid^2 \delta(\epsilon_{\mathbf{k}'} - \epsilon_{\mathbf{k}} - \hbar\omega_{\mathbf{k}'-\mathbf{k}}),$$

$$W_{emit} = \frac{2\pi}{\hbar} \frac{j_{ex}^2}{N} (n_{\mathbf{k}-\mathbf{k}'} + 1) \mid \langle \sigma' \mid c_{\downarrow}^{\dagger} c_{\uparrow} \mid \sigma \rangle \mid^2$$
$$\times \delta(\epsilon_{\mathbf{k}'} - \epsilon_{\mathbf{k}} + \hbar\omega_{\mathbf{k}-\mathbf{k}'}). \quad (C4)$$

Considering a scattering process in which the spin direction of initial electron locates at position α and the final electron at θ, namely $\mid \sigma \rangle = \mid \alpha \rangle$ and $\mid \sigma' \rangle = \mid \theta \rangle$, then the spin eigenfunctions of initial and final state in $\{\mid \uparrow \rangle, \mid \downarrow \rangle\}$ representation are found to be, respectively

$$\mid \alpha \rangle = \sin\left(\frac{\pi}{4} + \frac{\alpha - \phi}{2}\right) \mid \uparrow \rangle + \cos\left(\frac{\pi}{4} + \frac{\alpha - \phi}{2}\right) \mid \downarrow \rangle,$$

$$\mid \theta \rangle = \sin\left(\frac{\pi}{4} + \frac{\theta - \phi}{2}\right) \mid \uparrow \rangle + \cos\left(\frac{\pi}{4} + \frac{\theta - \phi}{2}\right) \mid \downarrow \rangle,$$
$$(C5)$$

where $\mid \uparrow \rangle$ ($\mid \downarrow \rangle$) denotes the state in which the spin direction is parallel (antiparallel) to the in-plane magnetization $\mathbf{M}$. Thus, we have

$$\mid \langle \theta \mid c_{\uparrow}^{\dagger} c_{\downarrow} \mid \alpha \rangle \mid^2 = \cos^2\left(\frac{\pi}{4} + \frac{\alpha - \phi}{2}\right)$$
$$\times \sin^2\left(\frac{\pi}{4} + \frac{\theta - \phi}{2}\right),$$

$$\mid \langle \theta \mid c_{\downarrow}^{\dagger} c_{\uparrow} \mid \alpha \rangle \mid^2 = \sin^2\left(\frac{\pi}{4} + \frac{\alpha - \phi}{2}\right)$$
$$\times \cos^2\left(\frac{\pi}{4} + \frac{\theta - \phi}{2}\right). \quad (C6)$$

For the two-dimensional case, we have the replacement $\sum_{\mathbf{k}'} = A/(2\pi)^2 \int d\mathbf{k}'$ in the continuum limit with A being the area of the sample. To deal with the integral $\int d\mathbf{k}$ for simplicity, a polar coordinate (γ, k_1), in which the original point is located at the Dirac cone point, namely $\mathbf{k}_0 = (m_y, -m_x)/v_F\hbar$, is introduced. Then, the vector $\mathbf{k}$ in the original coordinate is related to vector $\mathbf{k}_1$ in the new coordinate as

$$\mathbf{k} = \mathbf{k}_1 + \mathbf{k}_0 = \left(k_1\cos\gamma + \frac{m_y}{v_F\hbar}, k_1\sin\gamma - \frac{m_x}{v_F\hbar}\right). \quad (C7)$$

Thus, the band energy in Eq. (7) and the integrated form of $d\mathbf{k}$ are rewritten in the introduced polar coordinate, respectively, as

$$\epsilon_{\mathbf{k}} = \epsilon_{k_1} = nv_F\hbar k_1,$$
$$\epsilon_{\mathbf{k}} - E_f = nv_F\hbar k_1 - nv_F\hbar k_F = nv_F\hbar\Delta k,$$
$$\int d\mathbf{k} = \int d\mathbf{k}_1 = \int d\gamma \int k_1 dk_1 \approx k_F \int d\gamma \int dk_1, \quad (C8)$$

with Δk measured from k_F (Fermi wave number). After a series of derivation, $\tau_{mag}(\mathbf{k})$ [Eq. (C1)] is found to be

$$\frac{1}{\tau_{mag}(\mathbf{k})} = \frac{1}{\tau_{mag}^+(\mathbf{k})} + \frac{1}{\tau_{mag}^-(\mathbf{k})}, \quad (C9)$$

with the magnon scattering time $\tau_{mag}^+(\mathbf{k})$ [$\tau_{mag}^-(\mathbf{k})$] from the absorption (emission) process expressed as

$$\frac{1}{\tau_{mag}^+(\mathbf{k})} = \frac{1}{\tau_F^m} \int_0^{2\pi} d\theta \cos^2\left(\frac{\pi}{4} + \frac{\alpha - \phi}{2}\right)$$
$$\times \sin^2\left(\frac{\pi}{4} + \frac{\theta - \phi}{2}\right) V_{mag}^+(\theta, \alpha, \Delta k),$$

$$\frac{1}{\tau_{mag}^-(\mathbf{k})} = \frac{1}{\tau_F^m} \int_0^{2\pi} d\theta \sin^2\left(\frac{\pi}{4} + \frac{\alpha - \phi}{2}\right)$$
$$\times \cos^2\left(\frac{\pi}{4} + \frac{\theta - \phi}{2}\right) V_{mag}^-(\theta, \alpha, \Delta k), \quad (C10)$$

where $\frac{1}{\tau_F^m} = \frac{k_F j_{ex}^2 A_c}{2\pi v_F \hbar^2}$, and the formulas of $V_{mag}^+(\theta, \alpha, \Delta k)$ and $V_{mag}^-(\theta, \alpha, \Delta k)$ are given in Eqs. (13) and (14), respectively. According to Eqs. (C9) and (C10), one could easily observe that $\tau_{mag}(\mathbf{k})$ is a function of α and Δk. Hence, $\tau_{mag}(\mathbf{k})$ is written as $\tau_{mag}(\alpha, \Delta k)$ [Eq. (12)] in the main text.

In the polar coordinate $\mathbf{k}_1 = (\alpha, k_1)$, we have $\epsilon_{\mathbf{k}} = v_F\hbar|\mathbf{k}_1|$ and $\epsilon_{\mathbf{k}} - E_f = \hbar v_F\Delta k$, yielding

$$v_x = \frac{1}{\hbar}\frac{\partial\epsilon_k}{\partial k_x} = v_F\cos\alpha$$

$$v_y = \frac{1}{\hbar}\frac{\partial\epsilon_k}{\partial k_y} = v_F\sin\alpha,$$

$$\frac{\partial f_0}{\partial k_x} = -\frac{P}{(P+1)^2}\beta\hbar v_F\cos\alpha, \quad (C11)$$

$$\frac{\partial^2 f_0}{\partial k_x^2} \approx (\beta\hbar v_F)^2\frac{P(P-1)}{(P+1)^3}\cos^2\alpha,$$

where $P = e^{\beta(\epsilon_{\mathbf{k}}-E_f)} = e^{\beta\hbar v_F\Delta k}$ and we have assumed that $\beta\hbar v_F k_F \gg 1$. Substituting Eq. (C11) and $\tau_{mag}(\mathbf{k})$ [Eqs. (C9) and (C10)] into Eq. (11), we get

$$\alpha_{nl}^P = \frac{\gamma E_f^2 v_F \hbar}{k_B T^2} \int d\Delta k \int d\alpha \int d\theta V_{mag}(\theta, \alpha, \phi, \Delta k)$$
$$\times \frac{\cos^2\alpha \sin\alpha P}{(P+1)^2}\frac{\hbar v_F\Delta k}{k_B T}\left(\frac{P-1}{P+1}\frac{\hbar v_F\Delta k}{k_B T} - 2\right) \quad (C12)$$

with $\gamma = e j_{ex}^2 k_B(\tau^0)^3 A_c/(4\pi^3\hbar^5 v_F)$ and

$$V_{mag}(\theta, \alpha, \phi, \Delta k)$$
$$= \cos^2\left(\frac{\pi}{4} + \frac{\alpha - \phi}{2}\right)\sin^2\left(\frac{\pi}{4} + \frac{\theta - \phi}{2}\right)V_{mag}^+(\theta, \alpha, \Delta k)$$
$$+ \sin^2\left(\frac{\pi}{4} + \frac{\alpha - \phi}{2}\right)\cos^2\left(\frac{\pi}{4} + \frac{\theta - \phi}{2}\right)$$
$$\times V_{mag}^-(\theta, \alpha, \Delta k), \quad (C13)$$

where V_{mag}^+ and V_{mag}^- are given in Eqs. (13) and (14), respectively. When changing the integral variable Δk to x by the relation $x = v_F\hbar\Delta k/k_B T$ in Eq. (C13), one can easily

TABLE I. The parity properties about k_{1x} and k_{1y} for linear Dirac dispersion. The abbreviation "E" ("O") represent even (odd).

Transformation Function	$(-k_{1x}, -k_{1y})$ Parity	$(-k_{1x}, k_{1y})$ Parity	$(k_{1x}, -k_{1y})$ Parity
$\epsilon_{\mathbf{k}}$	E	E	E
v_x	O	O	E
v_y	O	E	O
$\frac{\partial f_0}{\partial k_x}$	O	O	E
$\frac{\partial^2 f_0}{\partial k_x^2}$	E	E	E

recover the formula of the nonlinear Nernst coefficient shown in Eq. (16).

APPENDIX D: PARITY PROPERTIES OF THE TERMS $[\epsilon_k, v_a, \partial f_0/\partial k_x$ AND $\partial^2 f_0/\partial k_x^2]$ FOR THE LINEAR DIRAC DISPERSION IN PRESENCE OF MAGNETIZATION

In presence of magnetization $\mathbf{M} = (m_x, m_y) = m\mathbf{e}_m$, the Dirac point and the whole dispersion will be shifted (see details in Sec. III). As discussed in Appendix C, when shifting the original point of the coordinate into the Dirac cone, locating at $\mathbf{k}_0 = (m_y, -m_x)/v_F\hbar$ in the original coordinate, the vector $\mathbf{k}_1$ in the new coordinate is related to the momentum $\mathbf{k}$ in the original coordinate as

$$k_{1x} = k_x - \frac{m_y}{v_F\hbar}, \quad k_{1y} = k_y + \frac{m_x}{v_F\hbar}. \quad (D1)$$

Therefore, the energy band $\epsilon_{\mathbf{k}}$ [Eq. (7)] is found to be $\epsilon_{\mathbf{k}} = nv_F\hbar k_1 = nv_F\hbar\sqrt{k_{1x}^2 + k_{1y}^2}$, hinting that ϵ_{k_1} is an even function with respect to k_{1x} (k_{1y}), namely $\epsilon(k_{1x}, k_{1y}) = \epsilon(-k_{1x}, k_{1y})$ and $\epsilon(k_{1x}, k_{1y}) = \epsilon(k_{1x}, -k_{1y})$. Correspondingly, the velocity $v_a = \frac{1}{\hbar}\frac{\partial\epsilon_{\mathbf{k}}}{\partial k_a}$, $\partial f_0/\partial k_x$ and $\partial^2 f_0/\partial k_x^2$ in the new coordinate can be expressed as

$$v_x = \frac{1}{\hbar}\frac{\partial\epsilon_{\mathbf{k}}}{\partial k_{1x}}, \quad v_y = \frac{1}{\hbar}\frac{\partial\epsilon_{\mathbf{k}}}{\partial k_{1y}}, \quad \frac{\partial f_0}{\partial k_x} = \frac{\partial f_0}{\partial k_{1x}}, \quad \frac{\partial^2 f_0}{\partial k_x^2} = \frac{\partial^2 f_0}{\partial k_{1x}^2}. \quad (D2)$$

Based on the parities of $\epsilon_{\mathbf{k}}$ in the new coordinate, the parities of functions (v_a, $\partial f_0/\partial k_x$ and $\partial^2 f_0/\partial k_x^2$) with respect to k_{1a} can be determined and are listed in Table I. Through exploiting the parities in Table I, one can easily find the terms in the first bracket in Eq. (10) are zero.

APPENDIX E: SYMMETRIC/ANTISYMMETRIC MAGNON SCATTERING TIME OF $1/\tau_{\text{mag}}$

In this Appendix, the origin of the $\cos\phi$ dependence of α_{nl}^P will be disclosed based on the symmetries (or parities) of the magnon scattering rate $1/\tau_{\text{mag}}$ with respect to k_{1y} in the new coordinate introduced in Appendix C. For simplicity, we neglect the magnon dispersion and take the magnon energy as $g\mu_B B$, then $V_{\text{mag}}^+(\theta, \alpha, \Delta k)$ [Eq. (13)] and $V_{\text{mag}}^-(\theta, \alpha, \Delta k)$ [Eq. (14)] no longer depend on θ and α and can be reexpressed as $V_{\text{mag}}^+(\Delta k)$ and $V_{\text{mag}}^-(\Delta k)$, respectively. Therefore, the magnon scattering rate $1/\tau_{\text{mag}}(\alpha, \Delta k)$ can be written as

$$\frac{1}{\tau_{\text{mag}}(\alpha, \Delta k)} = \frac{1}{\tau_F^m}\int_0^{2\pi}d\theta V_{\text{mag}}(\theta, \alpha, \phi, \Delta k)$$

$$= \int_0^{2\pi}\frac{d\theta}{\tau_F^m}\left[\cos^2\left(\frac{\pi}{4} + \frac{\alpha-\phi}{2}\right)\sin^2\left(\frac{\pi}{4} + \frac{\theta-\phi}{2}\right)V_{\text{mag}}^+(\Delta k) + \sin^2\left(\frac{\pi}{4} + \frac{\alpha-\phi}{2}\right)\cos^2\left(\frac{\pi}{4} + \frac{\theta-\phi}{2}\right)V_{\text{mag}}^-(\Delta k)\right]$$

$$= \frac{\pi}{2\tau_F^m}\{V_{\text{mag}}^+(\Delta k) + V_{\text{mag}}^-(\Delta k) + \sin(\phi-\alpha)\times[V_{\text{mag}}^+(\Delta k) - V_{\text{mag}}^-(\Delta k)]\}, \quad (E1)$$

The symmetry of τ_{mag} with respect to k_{1y} can be investigated through exploiting the parities of $\tau_{\text{mag}}(\alpha)$ when transforming α into $-\alpha$ in polar coordinate $(\alpha, \Delta k)$, where the polar angle α is measured from the k_{1x} and the radius Δk is measured from the Fermi momentum k_F. That is because the symmetry/antisymmetry of a function $f(k_{1x}, k_{1y})$ mean even/odd parities with respect to k_{1y}, namely $f(k_{1x}, k_{1y}) = f(k_{1x}, -k_{1y})/f(k_{1x}, k_{1y}) = -f(k_{1x}, -k_{1y})$, which corresponds to $f(\alpha) = f(-\alpha)/f(\alpha) = -f(-\alpha)$ in the polar coordinate. Therefore, the magnon scattering time $1/\tau_{\text{mag}}$ can be divided into two parts based on the parities on α,

$$\frac{1}{\tau_{\text{mag}}} = \frac{1}{\tau_{\text{mag}}^S} + \frac{1}{\tau_{\text{mag}}^A} \quad (E2)$$

with

$$\frac{1}{\tau_{\text{mag}}^S} = \frac{\pi}{2\tau_F^m}[(V_{\text{mag}}^+(\Delta k) + V_{\text{mag}}^-(\Delta k)) + (V_{\text{mag}}^+(\Delta k) - V_{\text{mag}}^-(\Delta k))\sin\phi\cos\alpha], \quad (E3)$$

and

$$\frac{1}{\tau_{\text{mag}}^A} = -\frac{\pi}{2\tau_F^m}[V_{\text{mag}}^+(\Delta k) - V_{\text{mag}}^-(\Delta k)]\cos\phi\sin\alpha, \quad (E4)$$

where superscripts "S"("A") refer to symmetry (antisymmetry). Equation (E3) [Eq. (E4)] hint that $\tau_{\text{mag}}^S[\tau_{\text{mag}}^A]$ is an even

[odd] function of k_{1y}, namely

$$\frac{1}{\tau_{\text{mag}}^S(k_{1x}, -k_{1y})} = \frac{1}{\tau_{\text{mag}}^S(k_{1x}, k_{1y})},$$

$$\frac{1}{\tau_{\text{mag}}^A(k_{1x}, -k_{1y})} = -\frac{1}{\tau_{\text{mag}}^A(k_{1x}, k_{1y})}. \quad (E5)$$

Besides, one can easily identify the terms in bracket in α_{nl}^P [Eq. (11)] are odd functions of k_{1y} when transforming the coordinate $\mathbf{k}$ into $\mathbf{k}_1$. Therefore, only the antisymmetric part

of magnon scattering time $1/\tau_{mag}^A$ ($\propto \cos\phi$) can give rise to nonzero Nernst coefficient α_{nl}^P, leading to a cosine dependence on the orientation of magnetization.

[1] M. Z. Hasan and C. L. Kane, Colloquium: Topological insulators, Rev. Mod. Phys. **82**, 3045 (2010).

[2] X.-L. Qi and S.-C. Zhang, Topological insulator and superconductors, Rev. Mod. Phys. **83**, 1057 (2011).

[3] S. A. Wolf, D. D. Awschalom, R. A. Buhrman, J. M. Daughton, S. V. Molnár, M. L. Roukes, A. Y. Chtchelanova, and D. M. Treger, Spintronics: A spin-based electronics version for the future, Science **294**, 1488 (2001).

[4] I. Žutić, J. Fabian, and S. D. Sarma, Spintronics: Fundamentals and application, Rev. Mod. Phys. **76**, 323 (2004).

[5] A. Fert, Nobel Lectures: Origin, development, and future of spintronics, Rev. Mod. Phys. **80**, 1517 (2008).

[6] D. Awschalom and N. Samarth, Spintronics without magnetism, Physics **2**, 50 (2009).

[7] Y. Ando, Topological insulator materials, J. Phys. Soc. Jpn. **82**, 102001 (2013).

[8] Y. Shiomi, K. Nomura, Y. Kajiwara, K. Eto, M. Novak, K. Segawa, Y. Ando, and E. Saitoh, Spin-electricity conversion induced by spin injection into topological insulator, Phys. Rev. Lett. **113**, 196601 (2014).

[9] R. Yu, W. Zhang, H.-J. Zhang, S.-C. Zhang, X. Dai, and Z. Fang, Quantized anomalous Hall effect in magnetic topological insulators, Science **329**, 61 (2010).

[10] C.-Z. Chang, J. Zhang, X. Feng, J. Shen, Z. Zhang, M. Guo, K. Li, Y. Ou, P. Wei, L.-L. Wang *et al.*, Experimental observation of the quantum anomalous Hall effect in a magnetic topological insulator, Science **340**, 167 (2013).

[11] X. Kou, S.-T. Guo, Y. Fan, L. Pan, M. Lang, Y. Jiang, Q. Shao, T. Nie, K. Murata, J. Tang, Y. Wang, L. He, T.-K. Lee, W.-L. Lee, and K. L. Wang, Scale-invariant quantum anomalous Hall effect in magnetic topological insulators beyond the two-dimensional limit, Phys. Rev. Lett. **113**, 137201 (2014).

[12] K. Yasuda, R. Wakatsuki, T. Morimoto, R. Yoshimi, A. Tsukazaki, K. S. Takahashi, M. Ezawa, M. Kawasaki, N. Nagaosa, and Y. Tokura, Geometric Hall effects in topological insulator heterostructures, Nat. Phys. **12**, 555 (2016).

[13] K. Yasuda, A. Tsukazaki, R. Yoshimi, K. S. Takahashi, M. Kawasaki, and Y. Tokura, Large unidirectional magnetoresistance in a magnetic topological insulator, Phys. Rev. Lett. **117**, 127202 (2016).

[14] S. R. Boona, R. C. Myers, and J. P. Heremans, Spin caloritronics, Energy Environ. Sci. **7**, 885 (2014).

[15] G. E. W. Bauer, A. H. MacDonald, and S. Maekawa, Spin caloritronics, Solid State Commun. **150**, 459 (2010).

[16] G. E. W. Bauer, E. Saitoh, and B. J. V. Wees, Spin caloritronics, Nat. Mater. **11**, 391 (2012).

[17] X.-Q. Yu, Z.-G. Zhu, G. Su, and A.-P. Jauho, Thermally driven pure spin and valley currents via the anomalous Nernst effect in monolayer group-VI dichalcogenides, Phys. Rev. Lett. **115**, 246601 (2015).

[18] X.-Q. Yu, Z.-G. Zhu, G. Su, and A.-P. Jauho, Spin-caloritronic, Phys. Rev. Appl. **8**, 054038 (2017).

[19] R. Watanabe, R. Yoshimi, M. Kawamura, M. Mogi, A. Tsukazaki, X. Z. Yu, K. Nakajima, K. S. Takahashi, and Y. Tokura, Quantum anomalous Hall effect driven by magnetic proximity coupling in all-telluride based heterostructure, Appl. Phys. Lett. **115**, 102403 (2019).

[20] Y. Deng, Y. Yu, M. Shi, Z. Guo, Z. Xu, J. Wang, X. Chen, and Y. Zhang, Quantum anomalous Hall effect in intrinsic magnetic topological insulator $MnBi_2Te_4$, Science **367**, 895 (2020).

[21] P. He, S. S.-L. Zhang, D. Zhu, Y. Liu, Y. Wang, J. Yu, G. Vignale, and H. Yang, Bilinear magnetoelectric resistance as a probe of three-dimensional spin-texture in topological surface state, Nat. Phys. **14**, 495 (2018).

[22] A. Dyrdal, J. Barnś, and A. Fert, Spin-momentum-locking inhomogeneities as a source of bilinear magnetoresistance in topological insulators, Phys. Rev. Lett. **124**, 046802 (2020).

[23] Y. Wang, B. Liu, Y.-X. Huang, S. V. Mambakkam, Y. Wang, S. A. Yang, X.-L. Sheng, S. A. Law, and J. Q. Xiao, Large bilinear magnetoresistance from Rashba spin-splitting on the surface of a topological insulator, Phys. Rev. B **106**, L241401 (2022).

[24] C. O. Avci, K. Garello, A. Ghosh, M. Gabureac, S. F. Alvarado, and P. Gambardella, Unidirectional spin Hall magnetoresistance in ferromagnet/normal metal bilayers, Nat. Phys. **11**, 570 (2015).

[25] T. Guillet, C. Zucchetti, Q. Barbedienne, A. Marty, G. Isella, L. Cagnon, C. Vergnaud, H. Jaffrès, N. Reyren, J.-M. George, A. Fert, and M. Jamet, Observation of large unidirectional Rashba magnetoresistance in Ge(111), Phys. Rev. Lett. **124**, 027201 (2020).

[26] J. Železný, Z. Fang, K. OlejnÍk, J. Patchett, F. Gerhard, C. Gould, L. W. Molenkamp, C. G. Olivella, J. Zemen, T. Tichý, T. Jungwirth, and C. Ciccarelli, Unidirectional magnetoresistance and spin-orbit torque in NiMnSb, Phys. Rev. B **104**, 054429 (2021).

[27] S. Shim, M. Mehraeen, J. Sklenar, J. Oh, J. Gibbons, H. Saglam, A. Hoffmann, S. S.-L. Zhang, and N. Mason, Unidirectional magnetoresistance in antiferromagnet/heavy-metal bilayers, Phys. Rev. X **12**, 021069 (2022).

[28] X.-Q. Yu, Z.-G. Zhu, and G. Su, Unidirectional Seebeck effect in magnetic topological insulators, Phys. Rev. B **100**, 195418 (2019).

[29] G.-H. Zhu, Y.-L. Wu, J.-L. Wan, and X.-Q. Yu, Unidirectional Seebeck effect from Rashba spin-orbit coupling on the subsurface of Ge(111), Phys. Rev. B **107**, 115430 (2023).

[30] K. Yasuda, A. Tsukazaki, R. Yoshimi, K. Kondou, K. S. Takahashi, Y. Otani, M. Kawasaki, and Y. Yokura, Current-nonlinear Hall effect and spin-orbit torque magnetization switching in a magnetic topological insulator, Phys. Rev. Lett. **119**, 137204 (2017).

[31] I. Sodemann and L. Fu, Quantum nonlinear Hall effect induced by Berry curvature dipole in time-reversal invariant materials, Phys. Rev. Lett. **115**, 216806 (2015).

[32] T. Low, Y. Jiang, and F. Guinea, Topological currents in black phosphorus with broken inversion symmetry, Phys. Rev. B **92**, 235447 (2015).

[33] Q. Ma, S.-Y. Xu, H. Shen, D. MacNeill, V. Fatemi, T.-R. Chang, A. M. M. Valdivia, S. Wu, Z. Du, C.-H. Hsu *et al.*, Observation of the nonlinear Hall effect under time-reversal-symmetric conditions, Nature (London) **565**, 337 (2019).

[34] Z. Z. Du, H.-Z. Lu, and X. C. Xie, Nonlinear Hall effects, Nat. Rev. Phys. **3**, 744 (2021).

[35] Y. Gao and D. Xiao, Orbital magnetic quadrupole moment and nonlinear anomalous thermoelectric transport, Phys. Rev. B **98**, 060402(R) (2018).

[36] X.-Q. Yu, Z.-G. Zhu, J.-S. You, T. Low, and G. Su, Topological nonlinear anomalous Nernst effect in strained transition metal dichalcogenides, Phys. Rev. B **99**, 201410(R) (2019).

[37] C. Zeng, S. Nandy, A. Taraphder, and S. Tewari, Nonlinear Nernst effect in bilayer WTe_2, Phys. Rev. B **100**, 245102 (2019).

[38] S. Korrapati, S. Nandy, and S. Tewari, Nonlinear thermoelectric response induced by Berry curvature quadrupole in systems with broken time-reversal symmetry, arXiv:2401.08155.

[39] X.-Q. Yu, Z.-G. Zhu, and G. Su, Hexagonal warping induced nonlinear planar Nernst effect in nonmagnetic topological insulators, Phys. Rev. B **103**, 035410 (2021).

[40] C.-C. Zeng, S. Nandy, and S. Tewari, Chiral anomaly induced nonlinear Nernst and thermal Hall effects in Weyl semimetals, Phys. Rev. B **105**, 125131 (2022).

[41] J. Zhang, C.-Z. Chang, Z. Zhang, J. Wen, X. Fang, K. Li, M. Liu, K. He, L. Wang, X. Chen *et al.*, Band structure engineering in $(Bi_{1−y}Sb_y)_2Te_3$ ternary topological insulators, Nat. Commun. **2**, 574 (2011).

[42] R. Yoshimi, A. Tsukazaki, Y. Kozuka, J. Falson, K. S. Takahashi, J. G. Checkelsky, N. Nagaosa, M. Kawasaki, and Y. Tokura, Quantum Hall states stabilized in semi-magnetic bilayers of topological insulators, Nat. Commun. **6**, 6627 (2015).

[43] C. Z. Chang, J. Zhang, M. Liu, Z. Zhang, X. Feng, K. Li, L.-L. Wang, X. Chen, X. Dai, Z. Fang *et al.*, Thin films of magnetically doped topological insulator with carrier-independent long-range ferromagnetic order, Adv. Mater. **25**, 1065 (2013).

[44] J. G. Checkelsky, R. Yoshimi, A. Tsukazaki, K. S. Takahashi, Y. Kozuka, J. Falson, M. Kawasaki, and Y. Tokura, Trajectory of the anomalous Hall effect towards the quantized state in a ferromagnetic topological insulator, Nat. Phys. **10**, 731 (2014).

[45] E. Erlandsen, A. Brataas, and A. Sudbø, Magnon-mediated superconductivity on the surface of a topological insulator, Phys. Rev. B **101**, 094503 (2020).

[46] K. Mæland, H. I. Røst, J. W. Wells, and A. Sudbø, Electron-magnon coupling and quasiparticle lifetimes on the surface of a topological insulator, Phys. Rev. B **104**, 125125 (2021).

[47] Y. Onose, T. Ideue, H. Katsura, Y. Shiomi, N. Nagaosa, and Y. Tokura, Observation of the magnon Hall effect, Science **329**, 297 (2010).

[48] Q. L. He, X. Kou, A. J. Grutter, G. Yin, L. Pan, X. Che, Y. Liu, T. Nie, B. Zhang, S. M. Disseler *et al.*, Tailoring exchange couplings in magnetic topological-insulator/antiferromagnet heterostructures, Nat. Mater. **16**, 94 (2017).

[49] N. V. Tarakina, S. Schreyeck, M. Duchamp, G. Karczewski, C. Gould, K. Brunner, R. E. Dunin-Borkowski, and L. W. Molenkamp, Microstructural characterization of Cr-doped $(Bi, Sb)_2Te_3$ thin films, Cryst. Eng. Commun. **19**, 3633 (2017).

[50] R. Yoshimi, A. Tsukazaki, K. Kikutake, J. G. Checkelsky, K. S. Takahashi, and Y. Tokura, Dirac electron states formed at the heterointerface between a topological insulator and a conventional semiconductor, Nat. Mater. **13**, 253 (2014).

[51] L. Yu, L. Hu, J. L. Barreda, T. Guan, X. He, K. Wu, Y. Li, and P. Xiong, Robust gapless surface state against surface magnetic impurities on $(Bi_{0.5}Sb_{0.5})_2Te_3$ evidenced by *in situ* magneto-transport measurements, Phys. Rev. Lett. **124**, 126601 (2020).

[52] Q. Liu, C.-X. Liu, C. Xu, X.-L. Qi, and S.-C. Zhang, Magnetic impurities on the surface of a topological insulator, Phys. Rev. Lett. **102**, 156603 (2009).

[53] J. Xu, W. A. Phelan, and C.-L. Chien, Large anomalous nernst effect in a van der Waals ferromagnet Fe_3GeTe_2, Nano Lett. **19**, 8250 (2019).

[54] K. Uchida, S. Takahashi, K. Harii, J. Ieda, W. Koshihae, K. Ando, S. Maekawa, and E. Saitoh, Observation of the spin Seebeck effect, Nature (London) **455**, 778 (2008).